ISSN : 1226-7244 (Print)
ISSN : 2288-243X (Online)
논문번호 22-03-20
j.inst.Korean.electr.electron.eng.Vol.26,No.3,475~482,September 2022
https://doi.org/10.7471/ikeee.2022.26.3.475
143

A Study on Two-Dimensional Variational Mode Decomposition Applied to Electrical Resistivity Tomography

Felipe Alberto Solano Sanchez*, Anil Kumar Khambampati*, Kyung Youn Kim*★

Abstract

Signal pre-processing and post-processing are some areas of study around electrical resistance tomography due to the low spatial resolution of pixel-based reconstructed images. In addition, methods that improve integrity and noise reduction are candidates for application in ERT. Lately, formulations of image processing methods provide new implementations and studies to improve the response against noise. For example, compact variational mode decomposition has recently shown good performance in image decomposition and segmentation. The results from this first approach of C-VMD to ERT show an improvement due to image segmentation, providing filtering of noise in the background and location of the target.

Key words : electrical resistivity tomography, post-processing, image segmentation, analytic signal, frequency spectrum

Ⅰ. Introduction

Electrical resistivity tomography(ERT) is a technique with wide applications in fields that vary from topography to medical diagnostics[1].

However in many measurements there is process noise on signals obtained from sensors[2]. This noise leads to artefacts in the background of output images, due to the ill-possedness of the reconstruction process. This condition can be reduced by regularization techniques or data processing methods[1].

On the side of data processing methods, algorithms as T-norm based linear back projection has been applied for cases of fluids phases. In this type of studies the final image precision is improved by the use of assumptions regarding the materials present in the flow[3]. However, these kind of assumptions are not possible for all the wide applications for ERT.

In the present study, an image decomposition and segmentation technique called two-dimensional compact variational mode decomposition(C-VMD) is introduced in the image post-processing of general ERT results.

By this post-processing, the ERT image result is decomposed into different modes, taking out the artefacts in background due to process noise and

* Department of Electronic Engineering, Jeju National University
★ Corresponding author
E-mail: kyungyk@jejunu.ac.kr, Tel : +82-64-754-3664
※ Acknowledgment
This research was supported by the 2022 scientific promotion program funded by Jeju National University
Manuscript received
Manuscript received Sep. 16, 2022; revised Sep 23, 2022; accepted Sep. 25, 2022.

leaving the defects to be detected. This final objective is achieved by extracting the different modes with a limited bandwidth regarding a characteristic center frequency.

II. Electrical Resistivity Tomography

Electrical resistivity tomography is an imaging technique in which electrodes are located at the boundary of an object(Ω) and measurements of potential(u) are done while applying alternating currents in a defined pattern. The measured potential is related to a conductivity distribution $\sigma(x,y)$ by[1]

$$\nabla \cdot (\sigma \nabla u) = 0, \quad \in \Omega \tag{1}$$

This partial differential equation is obtained by from relating Maxwell's equations in an inhomogeneous medium.

Different models have been developed for the solution of equation (1), such as the complete electrode model. This model stands out for the fact that it takes into account the interface between electrodes and the object in the study. It has been calculated and demonstrated that a surface impedance z_l is present at the mentioned interface. With this fact and a series of assumptions, the following boundary conditions are obtained [2, 4]

$$\int_{e_l} \sigma \frac{\partial u}{\partial v} dS = I_l \text{ on } e_l, l = 1,2,...,L \tag{2}$$

$$\sigma \frac{\partial u}{\partial v} = 0 \text{ on } x \in \partial\Omega \setminus \bigcup_{l=1}^{L} e_l \tag{3}$$

$$u + z_l \sigma \frac{\partial u}{\partial v} = U_l \text{ on } e_l, l = 1,2,...,L \tag{4}$$

Having e_l the area under the lth electrode, v as outward unit normal, I_l as the injected currents, L as the number of electrodes and U_l as the measured voltages at the boundary. Also, to ensure the existence and uniqueness of the solution, two restrictions are added

$$\sum_{l_1}^{L} I_l = 0 \tag{5}$$

$$\sum_{l_1}^{L} U_l = 0 \tag{6}$$

Because of difficulties in solving these equations in complex scenarios, a numerical procedure based on the finite element method(FEM) is used.

This method proceeds in first place with a mesh generation over the object(Ω) to solve what is called the "forward problem". In this, potential distribution(u) and voltages on electrodes(U) are approximated with[1]

$$u \approx u^h(x,y) = \sum_{i=1}^{N} \alpha_i \phi_i(x,y) \tag{7}$$

$$U \approx U^h = \sum_{j=1}^{L-1} \beta_i n_i \tag{8}$$

In which N is the number of nodes in FEM mesh, ϕ_i is a two-dimensional first-order basis function and n is the patterns for measurement as n_1=(1,-1,0,...,0)^T, n_2=(1,0,-1,...,0)^T $\in \mathbb{R}^L$. Unknowns to be determined are α_i and β_j, respectively, the nodal and boundary voltages. Using (7) and (8), the forward solution can be represented in a matrix equation

$$Ab = f \tag{9}$$

In which A is a sparse block matrix, b is the solution vector and f is a data vector. More details can be found at [1] regarding introduced matrices and FEM formulation.

III. 2-D VARIATIONAL MODE DECOMPOSITION

In this section, before explaining the 2-D VMD, it is convenient to introduce the concepts of analytic signal and the case of 1-D VMD.

1. Analytic Signal

By definition an analytic signal is composed of only positive frequency components. In the case of a 1-D space, an analytic signal is obtained by

the sum of a signal ($f(t)$) and its Hilbert Transform, defined as[5]

$$H\{f\}(t) = \frac{1}{\pi t} * f(t) = \frac{1}{\pi} P \int_{-\infty}^{\infty} \frac{f(\tau)}{t-\tau} d\tau \tag{9}$$

Having t as the time variable, P as the Cauchy principal value to ensure integral is not undefined and τ as a variable used for convolution. This formulation is equivalent to the convolution between $f(t)$ and $\frac{1}{t}$.

With this Hilbert transform result, the analytic signal is obtained in the time domain[6].

$$f(t)_{AS} = f(t) + jH\{f\}(t) \tag{10}$$

For the spectral domain, an analytic signal is obtained by taking out the negative frequencies[6]

$$f(\omega)_{AS} \begin{cases} 2f(\omega), & \text{if } \omega > 0 \\ f(\omega), & \text{if } \omega = 0 \\ 0, & \text{if } \omega < 0 \end{cases} \tag{11}$$

In the case of 2D signals, the same principle of frequency suppression on the spectral domain is used. To imitate the suppression of negative frequencies, a half-plane of the frequency domain is fixed to be zero, corresponding to a vector [6] ω_k.

$$f(\omega)_{AS} \begin{cases} 2f(\omega), & \text{if } \langle \omega, \omega_k \rangle > 0 \\ f(\omega), & \text{if } \langle \omega, \omega_k \rangle = 0 \\ 0, & \text{if } \langle \omega, \omega_k \rangle < 0 \end{cases} \tag{12}$$

2. Variational Mode Decomposition

The basic 1-D variational mode decomposition is based on theoretical concepts such as the Hilbert transform, analytic signals, heterodyne demodulation and Wiener filtering. These are combined to break down an input signal into different modes(u_k), each with a limited bandwidth around a central frequency (ω_k).

To define the bandwidth of the modes, the following process is used for each one[7]:

1. Calculate the analytic signal(with unilateral spectrum) using the Hilbert transform.

2. Modulate the signal to a baseband using the mode's central frequency.

3. Compute the mode's bandwidth through the Dirichlet energy of the demodulated signal.

By this, a constrained variational problem is obtained as[7]

$$\begin{aligned} u_k : \min_{\mathbb{R} \to \mathbb{R}, \omega_k} & \left\{ \sum_k \alpha_k \left\| \partial_t \left[\left\{ \left(\delta(t) + \frac{j}{\pi t} \right) * u_k(t) \right\} e^{-j\omega_k} \right] \right\|_2^2 \right\} \\ \text{s.t.} \quad & \forall t \in \mathbb{R} : \sum_k u_k(t) = f(t) \end{aligned} \tag{13}$$

With ω_k as the vector normal to the half plane that divides frequencies to be fixed to zero, α_k as a weighting parameter for each mode, $\delta(t)$ as Dirac delta function, j as an imaginary unit and u_k as the k'th mode.

It has been demonstrated that the use of this model exceeds other decomposition techniques with respect to modes separations and signal noise robustness[7, 8].

3. 2-D Variational Mode Decomposition

For the case of 2-D signals such as images, the previously exposed VMD can be generalized for n-dimensional spaces[8]

$$\begin{aligned} u_k : \min_{\mathbb{R}^n \to \mathbb{R}, \omega_k \in \mathbb{R}^n} & \left\{ \sum_k \alpha_k \left\| \nabla \left[u_{ASk}(x) e^{-j\langle \omega_k, x \rangle} \right] \right\|_2^2 \right\} \\ \text{s.t.} \quad & \forall x \in \mathbb{R}^n : \sum_k u_k(x) = f(x) \end{aligned} \tag{14}$$

With u_{ASk} as an analytic signal resulting from (12). Also, in the case of higher dimensions, the coefficient α_k allows the weighting for different k modes.

The reconstruction constraint is subject to a quadratic penalty, Lagrangian multiplier and a process around alternate direction minimization (ADMM). For more detail on these minimization schemes, refer to [7, 9].

4. Compact Variational Mode Decomposition

The intrinsic mode functions obtained in the

decompositions are assumed to have a slow variation in their spatial amplitude, far slower than the carrier wavelength[10].

Taking Carson's rule, the following is defined as an extension to apply for IMF's bandwidth[5].

$$BW_{AM-FM} := 2(\triangle f + f_{FM} + f_{AM}) \quad (15)$$

With $\triangle f$ as frequency swing and f_{FM} as modulation bandwidth of the FM component. Regarding f_{AM}, it is the AM component bandwidth.

This limitation of bandwidth can result on an incorrect separation of modes. To overcome this issue, a method of assigning binary support functions has been proposed in [7].

Ⅳ. Result and discussion

The present section presents results of ERT reconstructed images post-processing with C-VMD. Also, details regarding the various parameters and resulting metrics.

1. Image Reconstruction

EIDORS [11] libraries are used for image reconstruction in the Matlab software. As mentioned in section II, the package simulates a current pattern and measurements and proceeds with forward and inverse calculations.

For example, in Fig. 1-4, (a) and (b) represent the defined location of the defects and the image reconstruction respectively. The inverse problem is solved using modified Newton-Raphson (mNR) with $\alpha = 5 \times 10^6$.

2. Post-processing

Taking the reconstructed image as input, the C-VMD script presented in [6] is implemented for image segmentation. The main standard parameters used in all cases are shown in table 1.

Also on table 2, a summary of the different noise cases and results regarding iterations and ω_k convergence. As mentioned under section III, the ω_k parameter consist of a [x, y] vector that defines the plane for frequency filtering.

As commented in [12], one of the main pivots in VMD is the initialization and update of ω_k. This parameter highly dependents on the sub- signals coefficient for narrowbandedness(α). A high α value provides a finer separation of sub- signals, since the Wiener filter is concentrated around the correspondent central frequency. This drawback is that the central frequency may not contain critical information by not being a principal frequency.

On the other hand, a low value of α results in a broader filter, giving a better convergence for principal frequencies but with an inferior separation [12].

Table 1. Initial parameters for C-VMD.

Parameter	Definition	Value
Initial Alpha	subsignals coefficient for narrowbandedness	200
Beta	spatial mode support penalty coefficient	0.5
Gamma	spatial support TV-term	500
Delta	threshold for artifact classification	0.75
Rho	data fidelity coefficient	10
Rho_k	u-v signals splitting coefficient	10
Tau	time-step of dual ascent for data	2.5
Tau_k	time-step of dual ascent for u-v splitting	2.5
t	spatial support TV-term: time-step of ODE/PDE	2.5
K	number of modes to be recovered	3
DC	true for keeping first mode at DC	0
init	omegas initialization	0 (omegas initialized radially uniformly)
u_tol	tolerance for u convergence	1×10^{-8}
omega_tol	tolerance for omega convergence	1×10^{-8}
A_tol	tolerance for A convergence	0.0003
N	max number of iterations	250
A_phase	iterations for propagation phases	[100, inf]

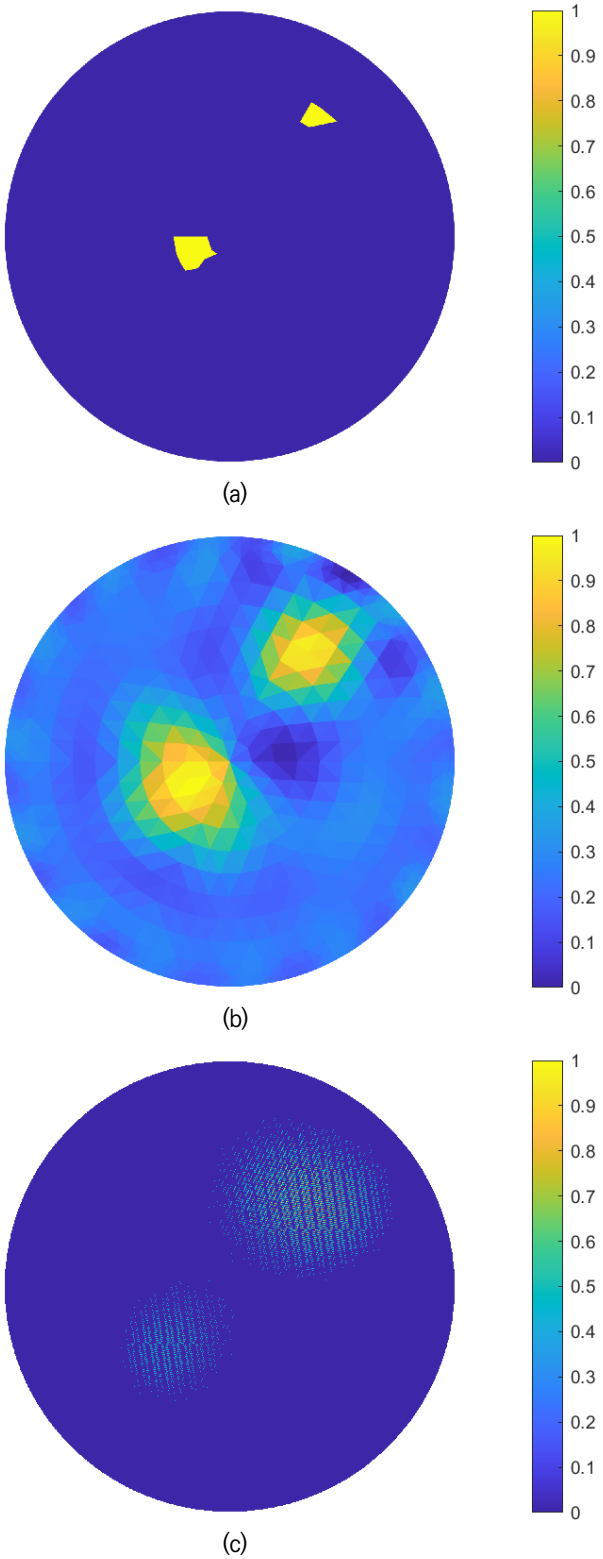

Fig. 1 Image reconstruction for numerical case 1 with no noise added to measurement signal.
(a) true distribution, (b) mNR output (c) C-VMD processing result.

Table 2. Cases with different SNR and corresponding C-VMD results.

	SNR	Iterations	Final ω_k values
Case 1	no noise	113	ω_1=[0.0747,0.0424] ω_2=[0.0275,0.1922] ω_3=[-0.216,0.0668]
Case 2	100	115	ω_1=[0.0738,0.0365] ω_2=[-0.0004,0.0746] ω_3=[-0.1444,0.0717]
Case 3	no noise	109	ω_1=[0.1404,0.0402] ω_2=[-0.0507,0.2216] ω_3=[-0.0674,0.0376]
Case 4	50	113	ω_1=[-0.1367,0.0826] ω_2=[0.1985,0.0619] ω_3=[-0.1051,0.0631]

Considering this, the C-VMD is modified to double the value for every ten iterations. This results in faster algorithm convergence since, without this modification, the used stopped criteria for an algorithm is the maximum number of iterations. It also shows a good performance on taking out background inhomogeneities, as seen in Fig. 1-4 (b) and (c).

Table 3. SSIM for presented cases.

	mNR	C-VMD
Case 1	0.6981	0.96
Case 2	0.6976	0.9592
Case 3	0.7286	0.9571
Case 4	0.6877	0.9535

Regarding metrics for the different used cases, table 3 summarizes the metric of structural similarity index (SSIM), which measures luminance, contrast, and structure of images between themselves[13].

Table 3 shows that according to the structural similarity index, the post-processed image has more similarity, which is the expected behavior since there is a denoised background space.

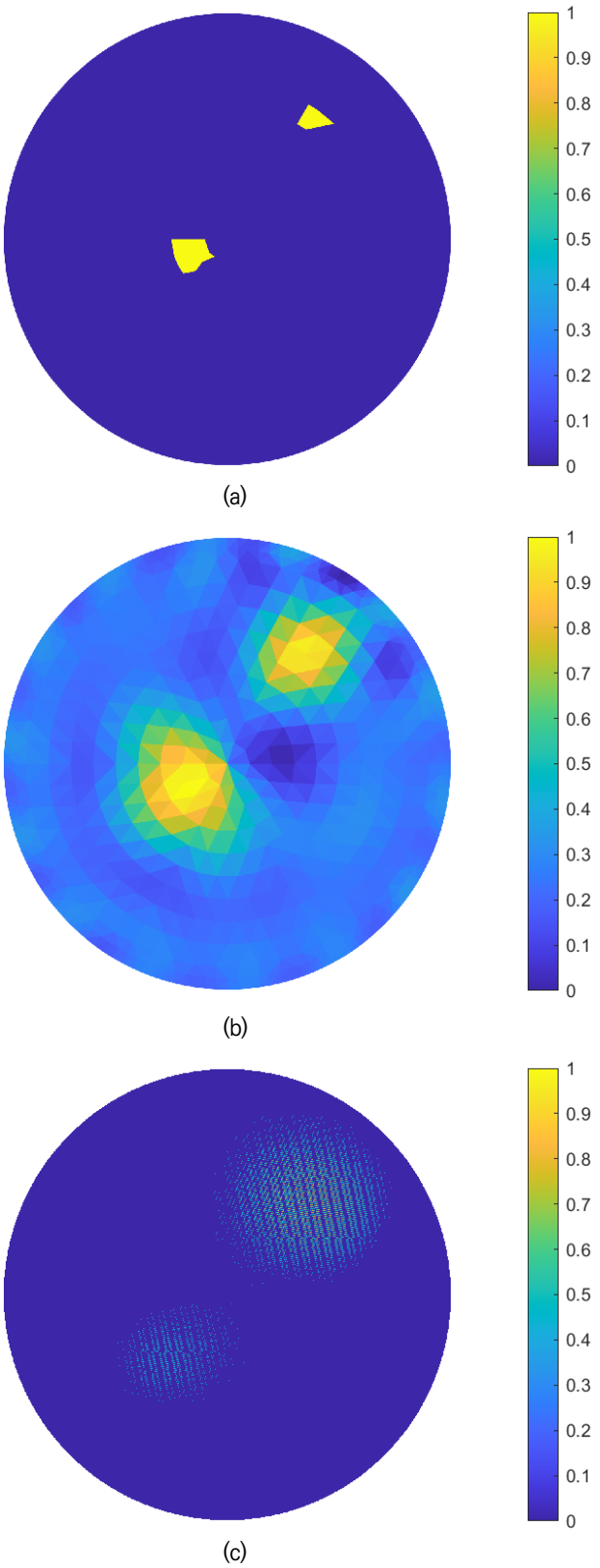

Fig. 2. Image reconstruction for numerical case 2 with SNR=50 added to measurement signal. (a) true distribution, (b) mNR output, (c) C-VMD processing result.

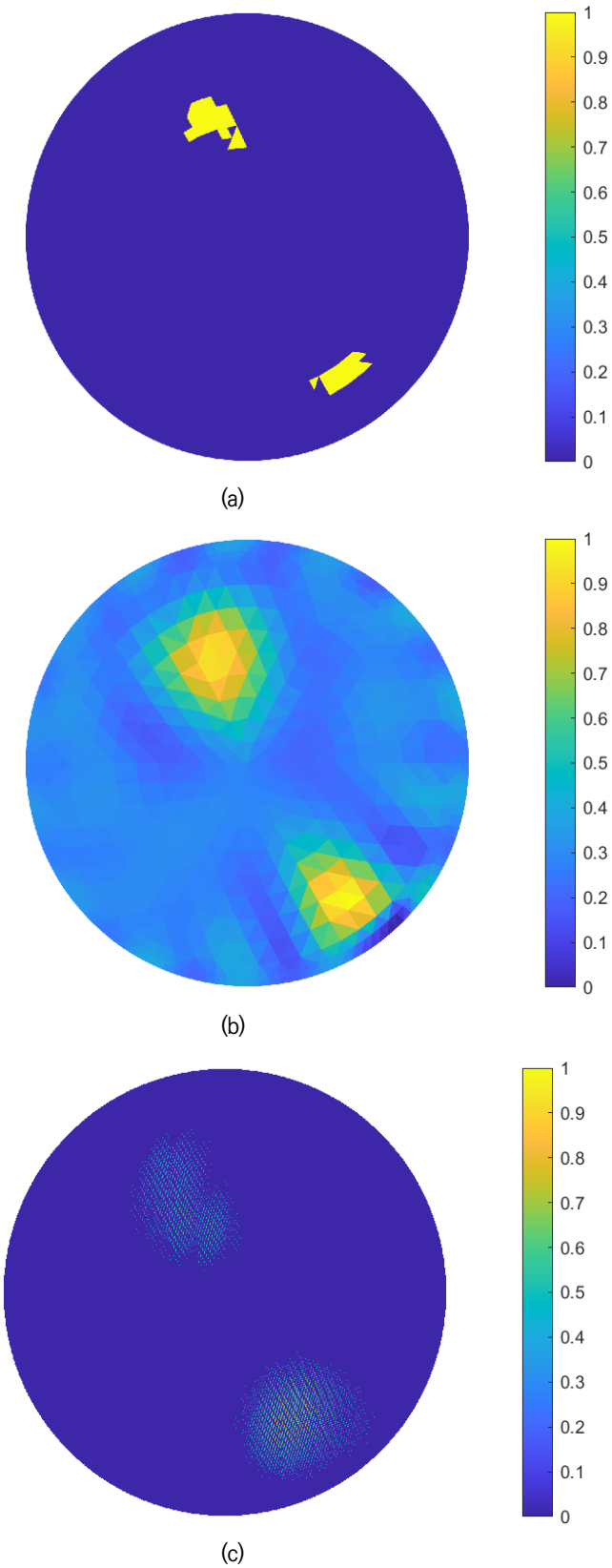

Fig. 3. Image reconstruction for numerical case 3 with no noise added to measurement signal. (a) true distribution, (b) mNR output, (c) C-VMD processing result.

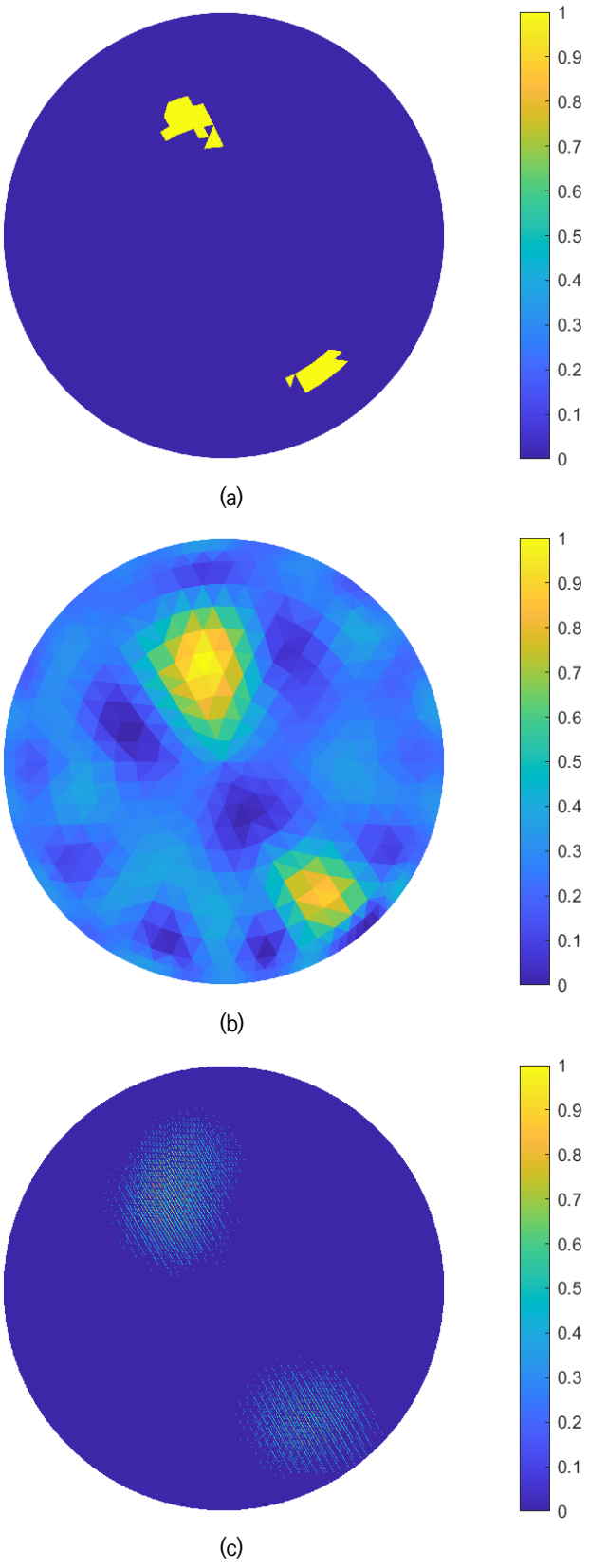

Fig. 4. Image reconstruction for numerical case 4 with SNR=50 added to measurement signal (a) true distribution, (b) mNR output, (c) C-VMD processing result.

V. Conclusions

This study presents the first compact variational mode decomposition approach to ERT processing. Since the number of variables to be tuned is significant, most of them are fixed to common values. Mostly the variables regarding frequency spectrum are studied since they provide considerable weight in the filtering behavior of the algorithm.

In further studies, these segmentation results can be combined with other areas, such as machine learning, to provide more variability to input data. Also, since the algorithm works on post-processing, it can be grouped with other processing methods or as a complement to other methods' outputs.

References

[1] M. Vauhkonen, "Electrical impedance tomography and prior information [Ph.D. thesis]," *University of Kuopio, Kuopio, Finland*, 1997. DOI: 10.1.1.208.9639

[2] G. Boverman, B. S. Kim, D. Isaacson and J. C. Newell, "The Complete Electrode Model For Imaging and Electrode Contact Compensation in Electrical Impedance Tomography," in 2009 *29th Annual International Conference of the IEEE Engineering in Medicine and Biology Society*, pp.3462-3465, 2009. DOI: 10.1109/IEMBS.2007.4353076.

[3] Z. Yang, Z. Li, S. Yue, M. Ding and J. Li, "An efficient LBP algorithm for ET imaging by reusing measurements," in 2018 *13th World Congress on Intelligent Control and Automation (WCICA)*, pp.1425-1429, 2018. DOI: 10.1109/WCICA.2018.8630469.

[4] L. Lu, L. Liu and C. Hu, "Analysis of the electrical impedance tomography algorithm based on finite element method and Tikhonov regularization," in 2014 *International Conference on Wavelet Analysis and Pattern Recognition*, pp.36-42, 2014. DOI: 10.1109/ICWAPR.2014.6961287.

[5] Huang, Norden & Shen, Zheng & Long, Steven

& Wu, M. L. C. & Shih, Hsing & Zheng, Quanan & Yen, Nai-Chyuan & Tung, Chi-Chao & Liu, Henry. "The empirical mode decomposition and the Hilbert spectrum for nonlinear and non-stationary time series analysis," in *Proceedings of the Royal Society of London. Series A: Mathematical, Physical and Engineering Sciences,* vol.454, pp.903-995, 1998. DOI: 10.1098/rspa.1998.0193.

[6] L. Cohen, "Time-frequency distributions-a review," in *Proceedings of the IEEE*, vol. 77, no.7, pp.941-981, 1989. DOI: 10.1109/5.30749.

[7] D. Zosso,K. Dragomiretskiy, A. L. Bertozzi, et al. "Two-Dimensional Compact Variational Mode Decomposition," *J Math Imaging*, Vis58, pp.294-320, 2017. DOI: 10.1007/s10851-017-0710-z

[8] K. Dragomiretskiy and D. Zosso, "Variational Mode Decomposition," in *IEEE Transactions on Signal Processing*, vol.62, no.3, pp.531-544, 2014. DOI: 10.1109/TSP.2013.2288675.

[9] D. P. Bertsekas, "Multiplier Methods: A Survey," in *IFAC Proceedings Volumes*, Vol.8, Issue.1, Part.1, pp.351-363, 1975.
DOI: 10.1016/S1474-6670(17)67759-0

[10] L. Cohen, "Time-frequency distributions-a review," in *Proceedings of the IEEE*, vol.77, no.7, pp.941-981, 1989, DOI: 10.1109/5.30749

[11] A. Adler and W. R. Lionheart, "Uses and abuses of eidors: an extensible software base for eit," in *Physiological measurement*, vol.27, no.5, p.S25, 2006. DOI: 10.1088/0967-3334/27/5/S03

[12] K. Dragomiretskiy, D. Zosso, "Two-Dimensional Variational Mode Decomposition," 2015.
DOI:10.1007/978-3-319-14612-6_15

[13] W. Zhou, A. C. Bovik, H. R. Sheikh, and E. P. Simoncelli. "Image Quality Assessment: From Error Visibility to Structural Similarity," in *IEEE Transactions on Image Processing*. Vol.13, Issue.4, pp.600-612, 2004. DOI: 10.1109/TIP.2003.819861.

BIOGRAPHY

Felipe Alberto Solano Sanchez (Member)

2020 : BE degree in Electronics, Technological Institute of Costa Rica, Costa Rica.

Anil Kumar Khambampati (Member)

2003 : BS degree in Mechanical Engineering, Jawaharlal Nehru Technological University, India.
2006 : MS degree in Marine Instrumentation Engineering, Jeju National University.
2010 : PhD degree in Electronic Engineering, Jeju National University.

Kyung Youn Kim (Member)

1983 : BS degree in Electronic Engineering, Kyungpook National University.
1986 : MS degree in Electronic Engineering, Kyungpook National University.
1990 : PhD degree in Electronic Engineering, Kyungpook National University.